ESS 951

Molecular Simulation, 1995, Vol. 14, pp. 259–274
Reprints available directly from the publisher
Photocopying permitted by license only

SIMULATING COMPLEX FLUIDS

K. ESSELINK, P.A.J. HILBERS, S. KARABORNI, J.I. SIEPMANN*
and B. SMIT†

*Shell Research B.V. Koninklijke/Shell-Laboratorium, Amsterdam, P.O. Box 38000
1030 BN Amsterdam The Netherlands*

(Received September 1993, accepted January 1995)

In this Article, a review is given on the progress of simulating complex fluids. Two approaches are used to deal with the special requirements of simulations of complex fluids. Molecular dynamics on massively parallel computers allow long simulations on very large systems. This makes it possible to simulate the self-assembly of micelles and the solubilization of a droplet of oil.

For problems in which dynamics is not essential, it is shown that a novel method, configurational-bias Monte Carlo, can be used to simulate efficiently systems containing chain molecules. The use of this method is illustrated by a calculation of the vapour-liquid curve of an alkane as long as octatetracontane C_{48}.

KEY WORDS: Complex fluids, parallel molecular dynamics, configurational-bias Monte Carlo, surfactant self-assembly, phase equilibria.

1 INTRODUCTION

Most of the systems of industrial importance would be considered as complex systems. Examples of such systems are polymers, liquid crystals, or surfactants. Computer simulations on these types of systems are much more demanding than simulations on simple fluids [1]. For example, if we use the molecular dynamics technique to study the properties of argon, the time required to generate a statistically independent configuration is approximately the time it requires for an atom to diffuse a distance of the order of its own diameter. For a chain molecule the required simulation time turned out to be much larger. Not only the distance the molecule has to diffuse—of the order of the radius of gyration of the molecule—is much larger but also the diffusion of a chain molecule is much slower.

In principle, the Monte Carlo method is not limited by the 'natural' time scale of the system. Monte Carlo moves can be developed which are impossible in nature but very efficient on a computer. An example of such a move is the displacement of a molecule to a random position in the system. The probability that such a move is accepted depends on the probability of finding an empty space, i.e. a new position of the particle that does not cause an overlap with the other particles. If for a mono-atomic particle this probability is approximately 1 out of 1000, the corresponding probability for a chain of

* Present address: Department of Chemistry, University of Minnesota, Minneapolis, MN 5455, USA
† Author for correspondence

n atoms would be 1 out of 1000^n. Clearly, such moves would only result in a reasonable acceptance rate for the shortest chain molecules.

In this Article, two approaches are discussed to simulate these complex fluids. For problems in which the dynamical behaviour is essential, one has to rely on the molecular dynamics technique. Progress will therefore depend on the development in computer power and the efficient use of massively parallel computers [2]. Here we show that these developments make it possible to study the self-assembly in surfactant systems. Furthermore some recent progress in Monte Carlo methods to simulate chain molecules is discussed [3,4]. For problems in which the dynamics is not of primary importance, these novel techniques turned out to be surprisingly efficient. The use of these methods is illustrated by simulations of phase equilibria of chain molecules.

2 SURFACTANT SELF-ASSEMBLY

A surfactant consists of a hydrophobic fragment chemically connected to a hydrophilic one. The amphiphilic nature of such molecules gives surfactants their unique properties. For example, added to water, surfactants reduce the surface tension and solubilize oil [5]. Besides these practical applications, surfactants are also of fundamental interest as model system to study self-assembly.

From a computer simulation point of view, surfactant behaviour is extremely difficult to study. This becomes clear if we consider the time scales involved in a micellar solution. Experimentally, it is estimated that it takes 10^{-8} to 10^{-6}s for a surfactant to leave or enter a micelle, that the fusion of two micelles occurs in a time span of 10^{-5} to 10^{-3}s, and that the lifetime of a micelle is of the order to 10^{-2} to 1s [6]. If we recall that a computer simulation, using the molecular dynamics technique, is limited to 10–100 nano seconds [1], it is obvious that drastic assumptions have to be made to study the self-assembly of micelles.

There have been two approaches to this problem. With a realistic model of a water/surfactant system it is necessary to construct the micelle à priori and study its evolution [7–12]. These simulations yield important information on the detailed structure of a micelle, but cannot be used, at present, to study the self-assembly of these micelles [13]. In this work, we focus on a complementary approach in which a very simple oil/water/surfactant model is studied. With such a simple model it turned out to be possible to observe the self-assembly process of micelles [14, 15], vesicles [16], and the solubilization of an oil droplet [17].

A. Oil/water/surfactant model

An important question one has to answer before one can construct a simple model of an oil/water/surfactant system is: what features of this sytem are responsible for the characteristic behaviour as is observed experimentally in these systems? Widom and co-workers were among the first to address this question [18–20]. Two simple observations constituted their starting point: oil and water do not mix, and a surfactant is an amphiphilic molecule, i.e. a molecule of which one side is hydrophilic and dislikes oil and the other side is hydrophobic and likes oil. Using these ingredients they

constructed a lattice model that predicted three-phase equilibria and ultra low surface tensions. Since then various other lattice models have appeared in the literature. A recent review of the results obtained by these lattice models is given in ref. [21]. Continuum models, based on the Widom model, have been developed by Stillinger [22], Wu *et al.* [23] and Telo da Gama and Gubbins [24].

In our model, which uses the same ingredients as the Widom model, we assume the existence of four types of particles: *o* particles, *w* particles, *h* particles, and *t* particles. These particles are used to model three types of molecules, namely oil molecules, water molecules and surfactant molecules. An oil molecule consists of a single *o* particle, and a water molecule consists of a single *w* particle. A surfactant molecule is made up of one or more *t* particles and one or more *h* particles; these are joined together by harmonic potentials

$$U_{ij} = \frac{1}{2} k(|\mathbf{r}_i - \mathbf{r}_j| - \sigma)^2, \tag{1}$$

where the value of the force constant is made sufficiently large such that at any instant 98% of the connected units have a length that is within 2% of the average value σ.

The four types of particles interact with truncated and shifted Lennard-Jones potentials with energy parameter ε_{ij}, distance parameter σ_{ij}, and the cut-off radius R_{ij}^c

$$\Phi_{ij} = \begin{cases} \phi_{ij}(r) - \phi_{ij}(R_{ij}^c) & r \leqslant R_{ij}^c \\ 0 & r > R_{ij}^c \end{cases}, \tag{2}$$

and

$$\phi_{ij}(r) = 4\varepsilon_{ij}\left[\left(\frac{\sigma_{ij}}{r}\right)^{12} - \left(\frac{\sigma_{ij}}{r}\right)^{6}\right], \tag{3}$$

where i, j indicates the type of atom (w, o, h or t) and r is the distance between the atoms. Of course, the use of a Lennard-Jones-type potential is a drastic simplification. Therefore, we have not tried to optimize the Lennard-Jones parameters for the various interactions. We have assumed that for all interactions $\varepsilon_{ij} = \varepsilon$ and $\sigma_{ij} = \sigma$. In order to make the *o*-*o* and *w*-*w* interactions different from the *w*-*o* interaction, the truncation of the potential (R_{ij}^c) is made depending on the type of interaction. The *w*-*w* and *o*-*o* interaction is truncated at $R_{ij}^c = 2.5\sigma$ and the *o*-*w* interaction at $R_{ij}^c = 2^{1/6}\sigma$, which makes the latter interaction completely repulsive. Furthermore, we have used for the *t* particles the same interactions as for the *o* particles. Therefore, the only difference between an *o* particle and a *t* particle is that the *t* particles are connected with harmonic forces (equation (1)) to other *t* or *h* particles (see Figure 1). The interactions of the *h* particles is for most surfactants identical to the interactions of the *w* particles. In order to study the effects of changing the interactions between head groups, we have used $R_{ij}^c = 2^{1/6}\sigma$ for the *h*-*h* interactions of some surfactants.

With these interactions, it turns out that at temperature $T = 1.0\,\varepsilon/k_B$ and density $\rho = 0.7\sigma^3$, the oil and water do not mix and form a stable liquid-liquid interface [25]. The surfactant molecules are of an amphiphilic nature, one end is hydrophilic (and dislikes oil), the other end is hydrophobic (and likes oil). With this model it is simple to mimic different chemical structures. For example, addition of oil-like particles to the

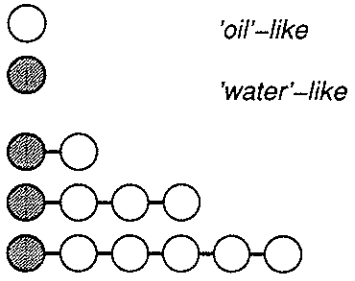

Figure 1 Schematic drawing of the oil/water/surfactant model.

tail allows us to study the influence of increasing the tail length [26] or branching of a surfactant [27].

B. Parallel molecular dynamics

To simulate large systems of particles for a large number of time steps, we have developed an efficient parallel molecular dynamics algorithm. In this section some aspects of the implementation are discussed.

Molecular dynamics is suited for being done on parallel computers since the computations are the same for many particles. There are two main techniques to exploit parallelism, viz. particle parallelism and geometric parallelism [28].

When particle parallelism is used, a fixed set of particles is assigned to a processor and these particles remain on this processor during the entire simulation [2, 29]. Continually, each processor calculates forces and the new positions for its particles. Since the distribution of particles remains unchanged during the simulation, it is straightforward to determine the assignments such that the workload is evenly distributed. The communication overhead can, however, become severe, since in order to evaluate the Lennard-Jones potentials it is necessary for each processor to communicate with all others to determine whether any two particles interact.

Geometric parallelism does not suffer from this particular disadvantage. It assigns space, not particles, to processors [30–32] (see Figure 2). During the computation, a processor calculates the trajectories of all particles it finds in its space. Because of the movement of the particles, some particles may enter a processor's space, others may leave. For this reason, processors continually need to redistribute the particles to make sure that each one has the right subset. Geometric parallelism can also efficiently be applied for evaluating multi-particle potentials such as bending and torsion potentials as is shown in [33].

The short range nature of the Lennard-Jones potential can be turned into a real advantage for geometric parallelism. Since the interactions in our model do not exceed distances larger than 2.5σ, it is not necessary to exchange information over long distances. This consideration has led to the well-known 'linked-list' method in which the simulation box is divided into a number of cells. These cells are assigned to a processor such that particles only interact with particles in the same cell or cells nearby (see ref. [1]). Furthermore, in our implementation we have used a combination

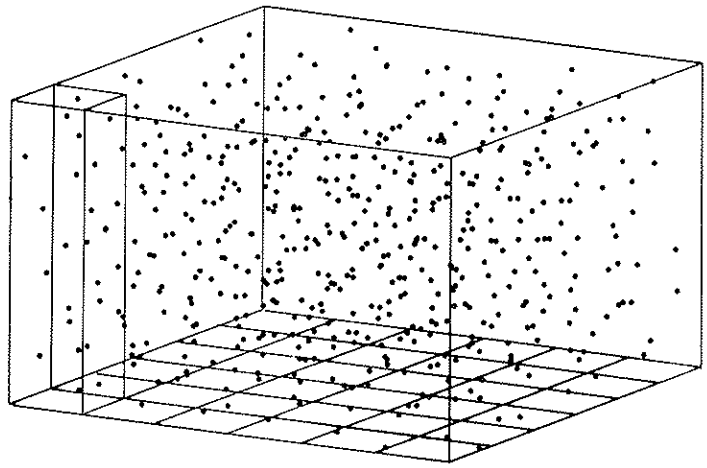

Figure 2 Schematic drawing of geometric parallelism. The squares on the bottom plane represent a torus network of 6*6 processors and the dots denote the particles. Each processor handles the particles in its own column.

of the neighbour list and linked list (see ref. [30] for details). The resulting algorithm scales linearly with the number of particles.

In Table I we present timing results of simulations done on a Cray X-MP (single processor), 36 and 400 T800 Transputers. We should note that the FORTRAN implementation for the Cray is fully vectorized. The timing results show that molecular dynamics simulations can benefit greatly from parallel computing, both in time and cost. Already for small numbers of particles a parallel machine can compete with a supercomputer as a Cray, but its real power is shown at large numbers of particles.

C. Results

The model introduced in the previous section contains many simplifications. It is therefore important to test whether this model still captures the essential properties of

Table 1 Comparison of execution times (seconds per iteration). ρ is the reduced density.

ρ	*#particles*	*Cray X-MP*	*36 T800*	*400 T800*
0.5	2916	0.11	0.48	0.10
0.7	4000	0.19	0.79	0.14
0.9	5324	0.32	1.47	0.23
1.0	6912	0.48	1.84	0.36
0.7	19652	1.05	—	0.41
0.7	32000	—	—	0.68
0.7	39304	2.05	—	0.86

surfactants, i.e. do the model surfactants lower the interfacial tension of the bare oil/water interface and do they self-assemble to form micelles?

1. The oil/water interface

In Figure 3, the effects of adding various types of model surfactants on the interfacial tension of the bare oil/water interface is shown [25, 26]. The figure shows that the model surfactants indeed lower the interfacial tension. Furthermore, increasing the tail length of the surfactants makes them more effective in reducing the interfacial tension. This is also found experimentally [26]. The reduction of the interfacial tension is in first approximation proportional to the number of surfactants at the interface. Deviation of this "ideal gas"-like behaviour makes surfactants more (or less) active. If the surfactants have longer tails, the effective size is larger and therefore they influence each other already at larger distances. This results in deviations of the ideal gas behaviour at smaller concentrations than for short chain surfactants.

These simulations demonstrated that the surface tension decreases linearly with surfactant concentration. In the experimental curves, a characteristic break in the interfacial tension is observed at high concentrations of surfactants. This is caused by the formation of micelles in the water phase. The simulations, on relatively small systems ($\approx$ 1000 particles), did not show the formation of micelles. Possible explanations include that the system is too small or that the model is too much simplified and does not contain those aspects that are essential for self-assembly.

2. Self-assembly

The study of self-assembly of micelles requires the use of very large systems. In refs. [14, 15, 34] simulations on 40,000 particles were performed on a parallel computer using the parallel molecular dynamics algorithm as discussed in section 2B. In Figure 4, a snapshot of a part of the system is shown. It is important to note that these

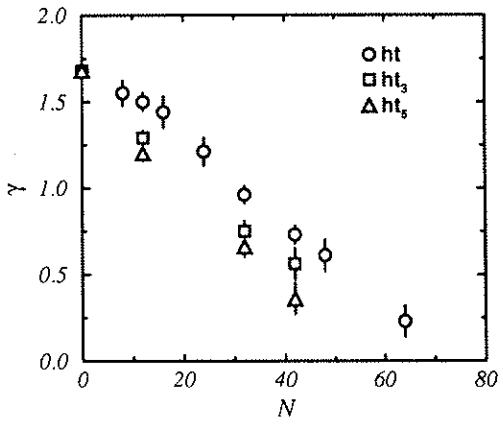

Figure 3 Surface tension γ as a function of the total number of surfactants N for various linear surfactants (the model of figure 1) as obtained from the simulations. The number of chain segments is ○: 1, □: 3, and Δ: 5. Details on the simulations can be found in ref. [25, 26].

simulations were started from a random distribution of surfactants. The monolayer and micelles were not constructed à priori. This figure shows that simulations on a simple surfactant model can be used to study the self-assembly of micelles.The micellar size distribution, a test for the system indeed being of micellar nature, has been calculated in ref. [15]. Furthermore, in these simulations one can observe the entering/leaving of surfactants into/from a micelle, the fusion of micelles, and even the break-down of a micelle. Similar processes have been observed experimentally [6].

The micelle morphology as a function of surfactant shape has been studied in ref. [35]. These simulations show that, depending on the size of the head group, one can observe bilayers, tubular micelles, or spherical micelles. The behaviour of amphiphilic

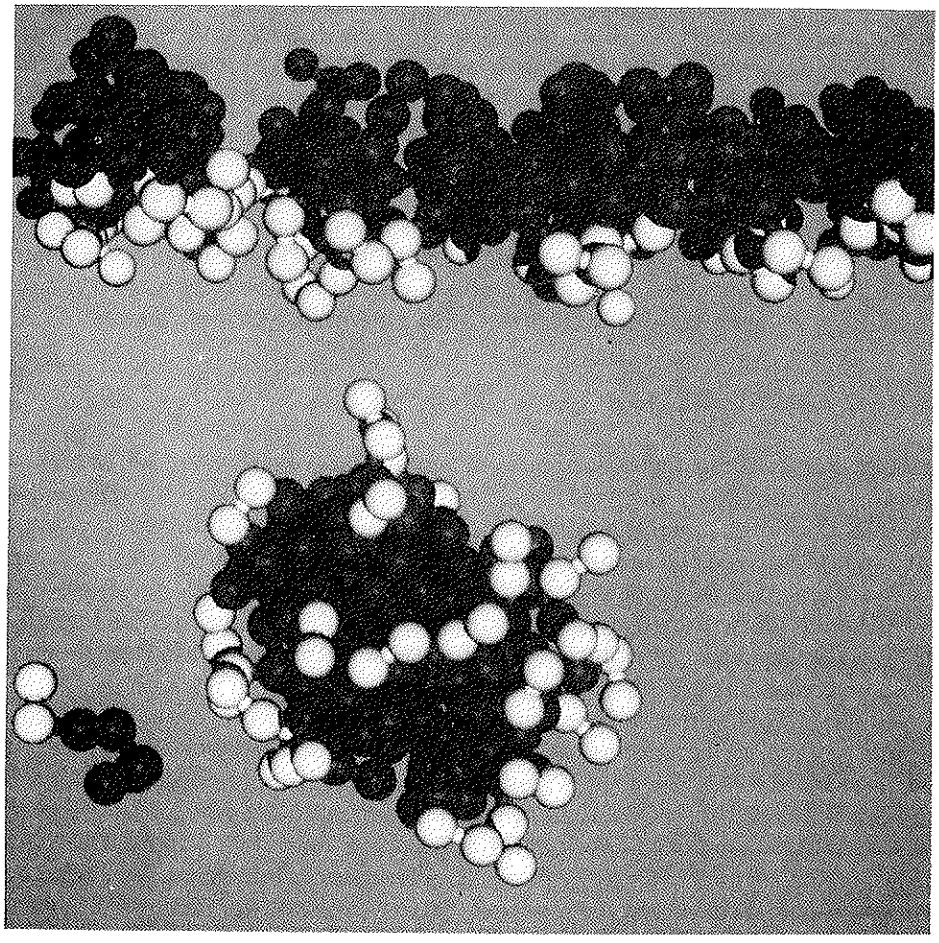

Figure 4 Typical example of a configuration of surfactants in an oil/water system for 1.5% surfactants. The total number of particles was ≈ 40,000. The snapshot shows some of the surfactants that form a monolayer at the oil/water interface and some surfactants in the water phase. For clarity, the surfactants in the oil phase and the oil and water particles are not shown. The hydrophilic segments are white and the hydrophobic segments red. Further details on these simulations can be found in refs. [14, 34]. (See Colour Plate 1.)

comb molecules in oil/water surfactant mixtures was studied by Balazs *et al.* [36] using a similar model. These calculations show the formation of intra-molecular polymer micelles. The self-assembly of vesicles has been studied by Drouffe *et al.* [16]. This work was focussed on the thermal fluctuations of vesicles.

3. Oil solubilization

From a technological point of view, the rate at which surfactants solubilize oil droplets is very important and has been studied extensively. The rational design of efficient surfactants requires a detailed understanding of the mechanism of oil solubilization. To obtain more understanding at a molecular level, molecular dynamics simulations have been performed to study the solubilization of an oil droplet in an aqueous surfactant solution [17]. This study, using the simple oil/water/surfactant model revealed three mechanisms for the transfer of oil molecules from the droplet to the water phase: (1) individual oil molecules leave the oil droplet and are trapped by micelles in the vicinity of the droplet, (2) the collision of the droplet with micelles causes the exchange of oil between the droplet and the micelle, and (3) because of the low interfacial tension between the oil droplet and the water, caused by the adsorption of surfactants, the oil droplet shows large fluctuations. During such a fluctuation part of the oil droplet together with a large number of surfactant molecules can desorb (see Figure 5). Furthermore, it is shown in ref. [17] that the extent to which either of these mechanisms prevails depends on the size of the oil molecules. For example, for small oil molecules mechanism (1) is more likely, while for large molecules the other two mechanisms are dominant.

3 PHASE EQUILIBRIA OF CHAIN MOLECULES

In the previous section, the self-assembly of a monolayer of surfactants at the oil-water interface and micelles in the water phase have been studied. One of the observations was that, as soon as the monolayer was formed, the transport of surfactants from the water phase through the monolayer into the oil phase became extremely slow. To enhance the equilibration, one would like to perform Monte Carlo moves in which a surfactant is taken from the water phase and inserted directly at a random position in the oil phase. As explained in the introduction, these type of moves for chain molecules results in a prohibitively low acceptance.

A similar problem arises in the calculation of phase equilibria of chain molecules. An efficient method to simulate vapour-liquid equilibria is the Gibbs-ensemble method of Panagiotopoulos [37, 38]. In this method, two boxes are simulated in parallel, one containing the vapour phase and the other the liquid phase. Monte Carlo moves ensure that the two boxes are in equilibrium with each other. Important is that the two boxes are not in direct contact, hence the presence of an interface is avoided. The coexistence properties can be calculated directly from these two boxes with a surprisingly small number of particles. The Monte Carlo moves that are used are (see Figure 6): displacement of particles, change of the volume of the boxes, and the exchange of particles between the two boxes. It is the last move, the exchange of particles, that makes the Gibbs ensemble difficult to apply on systems containing chain molecules. For example, at typical liquid conditions the probability of a successful insertion of

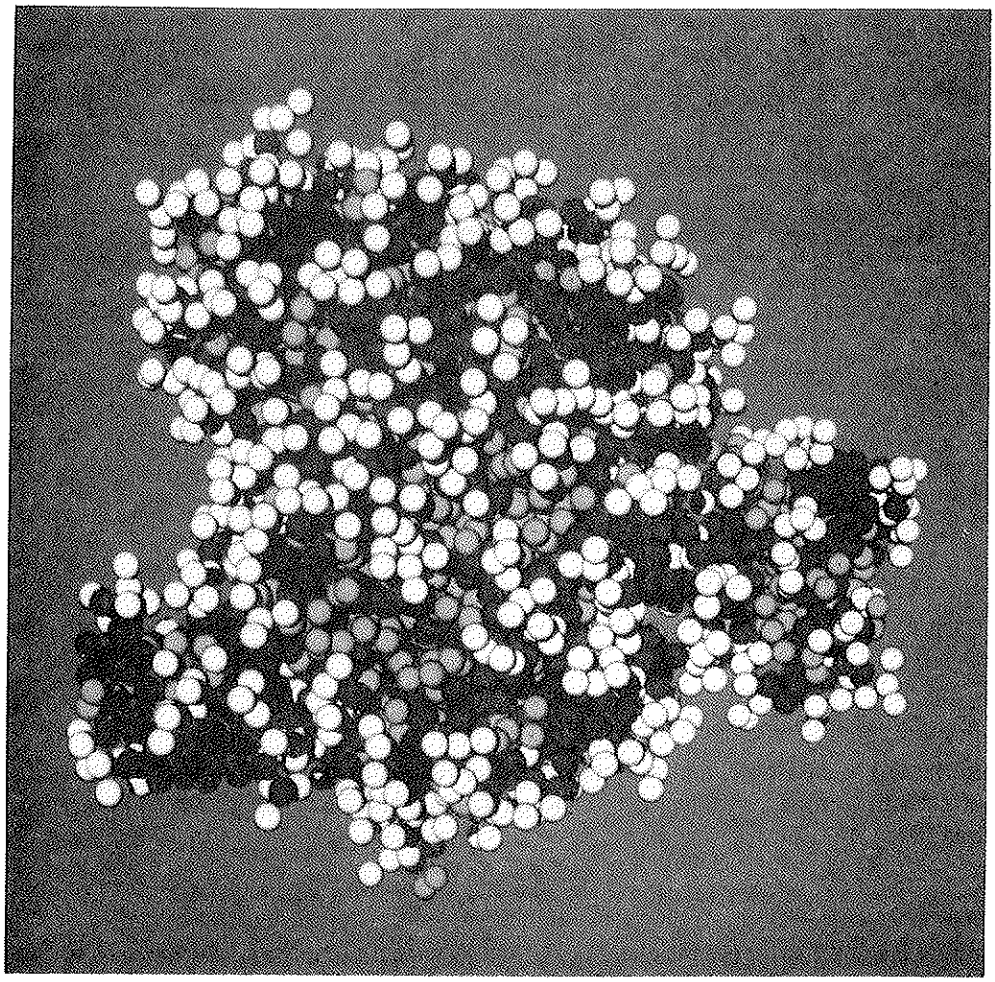

Figure 5 Instantaneous configuration of an oil droplet in water before the collective desorption of 26 surfactants and 26 oil molecules. Oil molecules are drawn in green, and surfactant molecules are drawn in red (tails) and white (headgroups). The water molecules are not shown. This figure is an illustration of mechanism (3) by which oil solubilization in micellar solutions proceeds. Details of mechanism (3) are mentioned in the text. Further details on these simulations can be found in ref. [17]. (See Colour Plate 2.)

a mono-atomic particle is of the order of 0.001. Therefore, for a chain this probability will again be extremely small. Configurational-bias Monte Carlo [3,4] has been developed to solve problems of this kind. Instead of a random insertion, the chain is grown atom by atom such that overlap with the other atoms is avoided. This growing introduces a bias which is removed by adjusting the acceptance rules [3,4]. The configurational-bias Monte Carlo technique has been applied successfully to study self-assembled monolayers [39,40]. In this Article, the use of configurational-bias Monte Carlo techniques is illustrated via calculations of phase equilibria of chain molecules [41] and *n*-alkanes [42–44].

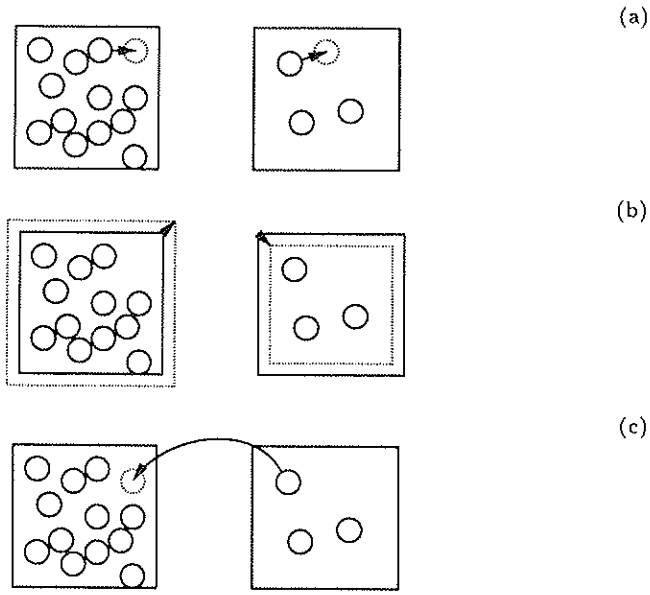

Figure 6 Monte Carlo moves in the Gibbs ensemble; (a) particle displacement (b) volume change, and (c) particle exchange.

A. Configurational-bias Monte Carlo

In the Gibbs ensemble, the probability of finding a configuration with n_1 particles in box 1 with volume V_1, and hence $N - n_1$ particles in box 2 with volume $V - V_1$ is given by [38]

$$\mathcal{N}(n_1, V_1) \propto \frac{V_1^{n_1}(V - V_1)^{N-n_1}}{n_1!(N-n_1)!} \exp(-\beta U_m), \tag{4}$$

where U_m is the total potential energy (sum of the energies of box 1 and box 2). In the Gibbs-ensemble method, configurations have to be generated which are distributed according to equation (4).

For systems with strong intra-molecular interactions, it is important to take these interactions into account while generating the trial conformation [4]. The potential energy of a given conformation of a molecule can be divided into two contributions:

(i) The *internal* potential energy (U^{int}), for an alkane this contribution would include bond-bending and torsion.
(ii) The *external* potential energy (U^{ext}) which takes into account the intermolecular interactions and those intra-molecular interactions which have not been taken into account in the internal part (for an alkane this would be the non-bonded interactions).

Note that this division is to some extent arbitrary and can be optimized for a given application. For the insertion of a chain in box 1, the following steps are carried out

1. for the first atom, a random position in box 1 is selected and the energy of this atom is calculated u_1^n

2. for the following atoms, a set k trial positions are generated. We denote these positions by $\{\mathbf{b}\} = (\mathbf{b}_1, \mathbf{b}_2, \ldots, \mathbf{b}_k)$ (see Figure 7). These positions are distributed on-the surface of a sphere. The radius of this sphere is equal to the bond length and the sphere is centered around the previously inserted atom of the chain. This set of trial orientations is generated using the internal part of the potential, which results in the following distribution for the l^{th} atom:

$$P_l(\mathbf{b}_i) = \frac{\exp[-\beta u_l^{n,\text{int}}(\mathbf{b}_i)]}{C}, \tag{5}$$

where $\beta = 1/k_B T$ and C is a normalization constant which is not important for the simulations. Note that this probability depends on which type of atom is being inserted. Of each of these trial positions the external energy is calculated with the atoms of the other molecules and with those atoms of the molecule that are already grown, $u_l^{n,\text{ext}}(\mathbf{b}_j)$, and one of these positions is selected with a probability

$$p(l) = \frac{\exp[-\beta u_l^{n,\text{ext}}(\mathbf{b}_j)]}{w^{n,\text{ext}}(l)}, \tag{6}$$

in which

$$w^{n,\text{ext}}(l) = \sum_{j=1}^{k} \exp[-\beta u_l^{n,\text{ext}}(\mathbf{b}_j)]. \tag{7}$$

3. after repeating step 2 till the entire chain of length M has been grown, we calculate

$$W^n = \exp[-\beta u^{n,\text{ext}}(1)] \prod_{l=2}^{M} w^{n,\text{ext}}(l). \tag{8}$$

If a chain has been grown successfully in box 1, we continue by considering box 2 from which a randomly selected molecule has to be deleted.

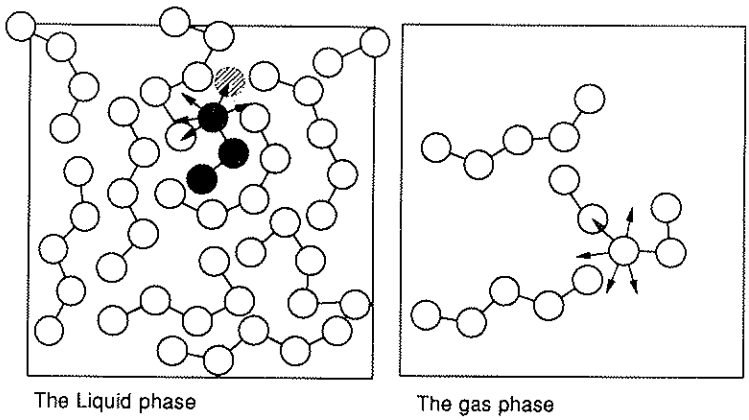

Figure 7 Schematic drawing of the configurational-bias Monte Carlo algorithm. The figure shows an attempt to exchange a particle from the gas phase into the liquid phase. Of the shaded chain 3 segments have been grown successfully and to insert the 4th segment k trial positions are generated (indicated by arrows). Figure adopted from ref. [43].

1. the energy of the first atom is calculated $u^{o,\mathrm{ext}}(1)$
2. for the following atoms, the external energy is calculated $u^{o,\mathrm{ext}}(l)$ and a set of $k-1$ trial orientations is generated with a probability given by equation (5). Note that also in this case the probability depends on the type of atom being considered. Using this set of orientations and the actual position, we calculated for atom l

$$w^{o,\mathrm{ext}}(l) = \exp[-\beta u^{o,\mathrm{ext}}(l)] + \sum_{j=2}^{k} \exp[-\beta u^{o,\mathrm{ext}}(\mathbf{b}_j)]. \tag{9}$$

3. after repeating step 2 till all M atoms of the chain have been considered, we calculate for the entire molecule

$$W^o = \exp[-\beta u^{o,\mathrm{ext}}(1)] \prod_{l=2}^{M} w^{o,\mathrm{ext}}(l). \tag{10}$$

Finally, the move is accepted with a probability

$$\mathrm{acc}(o|n) = \min\left(1, \frac{n_1(V - V_1)}{(N - n_1 + 1)\, V_1} \frac{W^n}{W^o}\right). \tag{11}$$

We continue by showing that this acceptance rule indeed removes the bias of the growing process. Consider the rate of transformations from o to n, where o is a state with n_1 molecules in box 1 with volume V_1 and state n has $n_1 + 1$ molecules in box 1 with the same volume. This rate is the product of the probability of being in state o, the probability of generating configuration n, and the acceptance of the move, or

$$K(o|n) = \mathcal{N}(\mathrm{o}) P(o|n) \mathrm{acc}(o|n). \tag{12}$$

The probability of generating configuration n is (combine equations (5) and (6) and use equation (8)),

$$\begin{aligned} P(o|n) &= \prod_{l=2}^{M} P_l(\mathbf{b}_i) p(l) \\ &= \prod_{l=2}^{M} \frac{\exp[-\beta u_l^{n,\mathrm{int}}(\mathbf{b}_i)]}{C} \frac{\exp[-\beta u_l^{n,\mathrm{ext}}(\mathbf{b}_j)]}{w^{n,\mathrm{ext}}(l)} \\ &= \exp(-\beta u^n) \frac{1}{C^{M-1}} \frac{1}{W^n}, \end{aligned} \tag{13}$$

where u^n is the total energy of the chain. In these equations we have used that the total energy of the molecule can be written as

$$u = u^{\mathrm{ext}} + u^{\mathrm{int}} = \sum_{l=1}^{M} [u^{\mathrm{ext}}(l) + u^{\mathrm{int}}(l)]. \tag{14}$$

For the reverse move, the rate of transformations from n to o we can write

$$K(n|o) = \mathcal{N}(n) P(n|o) \mathrm{acc}(n|o). \tag{15}$$

The probability of generating these configurations is (compare equation (13))

$$P(n|o) = \exp(-\beta u^o)\frac{1}{C^{M-1}}\frac{1}{W^o}. \tag{16}$$

If we demand detailed balance ($K(o|n) = K(n|o)$) and take the pseudo- Boltzmann distribution for $\mathcal{N}$, equation (4), we arrive at the following condition for the ratio of the acceptance rules

$$\frac{\text{acc}(o|n)}{\text{acc}(n|o)} = \frac{n_1(V-V_1)}{(N-n_1+1)V_1}\frac{W^n}{W^o}. \tag{17}$$

Since equation (11) satisfies this condition, we have demonstrated that the above scheme obeys detailed balanced and the correct distribution of conformation is generated.[1]

B. Results

In Figure 8 the vapour liquid curve of an 8 bead Lennard-Jones chain is shown [41]. The beads are connected by bonds of a fixed length σ and bonds are allowed to rotate freely with respect to each other. The monomer-monomer interaction is modeled by a Lennard-Jones potential that is cutoff at a radius $R_c = 2.5\sigma$ and shifted. Compared to the mono-atomic Lennard-Jones fluid, the critical temperature of the chain is higher: $T_c^* = 2.07$ compared to $T_c^* = 1.09$, and the critical density is slightly lower: $\rho_c^* = 0.22$ compared to $\rho_c^* = 0.3$. It is important to note that, using the conventional insertion techniques, such simulations would necessitate billions of years of super computer time.

These type of simulations are not limited to model chain molecules and can also be applied to calculate the vapour-liquid curve of realistic models of molecules [42–44]. In

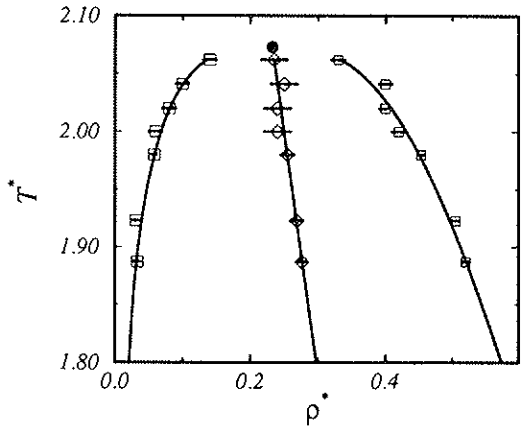

Figure 8 Liquid-vapour coexistence curve of a system of 200 chains of 8 Lennard-Jones monomers. The monomer-monomer interaction is modeled by a Lennard-Jones potential that is cutoff at a radius $R_c = 2.5\sigma$ and shifted. $T^* = kT/\varepsilon$ and $\rho^* = \rho/\sigma^3$. The estimate of the critical point is indicated by a black dot. Figure adopted from ref. [41].

[1] For clarity we have omitted in the proof some technical details. A complete proof can be found in ref. [4].

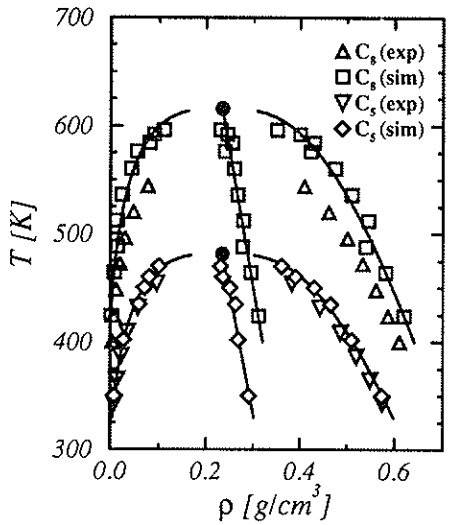

Figure 9 Vapour-liquid equilibria of pentane (lower curves) and octane (upper curves). Δ, ∇ are the experimental data of octane and pentane, respectively [47]. The simulation results are denoted by □ for octane and ◇ for pentane. The solid lines are the fits to the scaling law and the rectilinear law. ● is the estimate of the critical point as obtained from these fits. Figure adopted from ref. [44].

Figure 9, the calculated vapour-liquid curves of *n*-pentane and *n*-octane are shown. The calculations were performed for a united-atom model using the OPLS-parameter set of Jorgensen and co-workers [45]. It turned out that these calculations are not limited to very short alkanes, but can be used to calculate the phase diagram of an *n*-alkane as long as octatetracontane (C_{48}) (see Figure 10). Since the alkanes are thermally unstable above approximately 650 K, experimental data of C_{48} does not exist. Yet, these long chain alkanes do occur in mixtures of industrial importance and therefore the critical properties of these molecules are essential in the design of petrochemical processes,

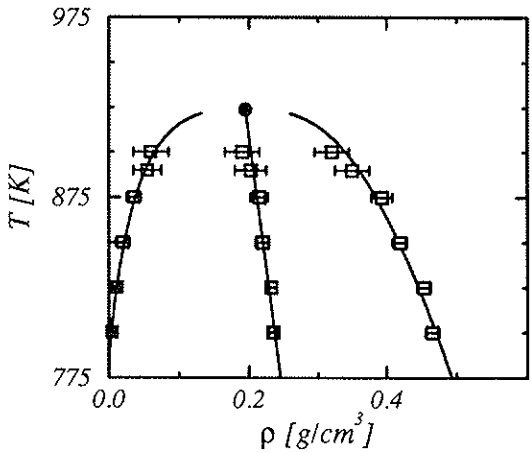

Figure 10 Gibbs-ensemble simulations of the vapour-liquid equilibria of octatetracontane C_{48}. Figure adopted from ref. [43].

even if they are unstable close to the critical point [46]. These results show that simulations can be used as an "engineering-tool" to estimate properties that can not be quantified with any other technique.

4 CONCLUDING REMARKS

In this article, some recent progress in the simulations of complex fluids is reviewed. It is shown that the use of massively parallel computers allows us to study the self-assembly of micelles and the solubilization of an oil droplet. This development shows that it is possible to perform systematic studies on these systems. This may lead to a better understanding of processes involving surfactants, which range from detergency to the transport through biological membranes.

Parallel to these developments in molecular dynamics, the development of efficient Monte Carlo methods to simulate chain molecules will be of importance in many applications. Here this technique is applied to simulate phase equilibria of *n*-alkanes, but these techniques are in no way limited to these molecules and can be used in many other applications of complex fluids.

References

[1] M.P. Allen and D.J. Tildesley. *Computer Simulation of Liquids*, Clarendon, Oxford, 1987.
[2] D. Fincham. Parallel computers and molecular simulation. *Mol. Sim.* 1, 1 45 (1987)
[3] J.I. Siepmann and D. Frenkel. Configurational-bias Monte Carlo: a new sampling scheme for flexible chains. *Mol. Phys.* **75**, 59–70 (1992).
[4] D. Frenkel, G.C.A.M. Mooij and B. Smit. Novel scheme to study structural and thermal properties of continuously deformable molecules. *J. Phys.: Condens. Matter* **4**, 3053–3070 (1992).
[5] K.L. Mittal and B. Lindman eds, *Surfactants in Solution*, Plenum, New York, 1984.
[6] J. Lang and R. Zana. "Chemical relaxation methods," In *Surfactants in Solution: new methods of investigation*, R. Zana, editor, New York, 1987, Dekker.
[7] S.W. Hann and L.R. Pratt. Monte Carlo study of a simple model for micelle structure. *Chem. Phys. Lett.* **79**, 430–440 (1981).
[8] J.M. Haile and J.P. O'Connell. Internal structure of a model micelle via computer simulation. *J. Phys. Chem.* **88**, 6363–6366 (1984).
[9] S. Karaborni and J.P. O'Connell. Molecular dynamics simulations of model micelles. 3. Effects of various intermolecular potentials. *Langmuir* **6**, 905 (1990).
[10] B. Jönsson, O. Edholm and O.J. Teleman. Molecular dynamics simulations of a sodium octanoate micelle in aqueous solution. *J. Chem. Phys.* **85**, 2259–2271 (1986).
[11] K. Watanabe and M.L. Klein. Shape fluctuations in ionic micelles. *J. Phys. Chem.* **93**, 6897–6901 (1989).
[12] J.C. Shelley, M. Sprik and M.L. Klein. Molecular dynamics simulations of an aqueous sodium octanoate micelle using polarizable surfactant molecules. *Langmuir* **9**, 916–926 (1993).
[13] B. Smit. "Computer simulations of surfactants." In *Computer simulation in Chemical Physics*, M.P. Allen and D.J. Tildesley, editors, 461–472, Dordrecht, 1993. NATO ASI, Kluwer.
[14] B. Smit, P.A.J. Hilbers, K. Esselink, L.A.M. Rupert, N.M. van Os and A.G. Schlijper. The structure of the water/oil interface in the presence of micelles. *Nature* **348**, 624–625 (1990).
[15] B. Smit, K. Esselink, P.A.J. Hilbers, N.M. van Os and I. Szleifer. Computer simulations of surfactant self-assembly. *Langmuir* **9**, 9–11 (1993).
[16] J.M. Drouffe, A.C. Maggs and S. Leibler. Computer simulations of self-assembled membranes. *Science* **254**, 1353–254 (1991).
[17] S. Karaboni, N.M. van Os, K. Esselink and P.A.J. Hilbers. Molecular dynamics simulations of oil solubilization in surfactant solution. *Langmuir* **9**, 1175–1178 (1993).
[18] J.C. Wheeler and B. Widom. Phase transitions and critical points in a model three-component system. *J. Am. Chem. Soc.* **90**, 3064 (1968).

[19] B. Widom. Lattice-gas model of amphiphiles and of their orientation at interfaces. *J. Phys. Chem.* **88**, 6508–6514 (1984).
[20] B. Widom. Phase transitions in surfactant solutions and in their interfaces. *Langmuir* **3**, 12–17 (1987).
[21] G. Gompper and M. Schick. "Lattice theories of microemulsions." In *Modern Ideas and Problems in Amphiphilic Science*, W.M. Gelbart, D. Roux and A. Ben-Shaul, editors, Berlin, in press. Springer.
[22] F.H. Stillinger. Variational model for micelle structure. *J. Chem. Phys.* **78**, 4654–4661 (1983).
[23] D. Wu, D. Chandler and B. Smit. Electrostatic analogy for surfactant assemblies. *J. Phys. Chem.* **96**, 4077–4083 (1992).
[24] M.M. Telo da Gama and K.E. Gubbins. Adsorption and orientation of amphiphilic molecules at a liquid–liquid interface. *Mol. Phys.* **59**, 227–239 (1986).
[25] B. Smit. Molecular dynamics simulations of amphiphilic molecules at a liquid–liquid interface. *Phys. Rev. A* **37**, 3431–3433 (1988).
[26] B. Smit, A.G. Schlijper, L.A.M. Rupert and N.M. van Os. Effects of chain length of surfactnats on the interfacial tension: Molecular dynamics simulations and experiments. *J. Phys. Chem.* **94**, 6934–6935 (1990).
[27] B. Smit. Computer Simulation of Phase Coexistence: from Atoms to Surfactants Ph.D. thesis, Rijksuniversiteit Utrecht, The Netherlands, 1990.
[28] P.A.J. Hilbers and K. Esselink. "Parallel computing and molecular dynamics simulations." In *Computer simulation in Chemical Physics*, M.P. Allen and D.J. Tildesley, editors, 473–495, Dordrecht, 1993. NATO ASI, Kluwer.
[29] J. Li, D.J. Brass, D.J. Ward and B. Robson. A study of parallel molecular dynamics algorithms for N-body simulations on a transputer system. *Par. Comp.* **14**, 211–222 (1990).
[30] K. Esselink, B. Smit and P.A.J. Hilbers. Efficient parallel implementation of molecular dynamics on a toroidal network: Part I parallelizing Strategy *J. Comp. Phys.* **106**, 101–107 (1993).
[31] H.G. Petersen, S.W. De Leeuw and J.W. Perram. Molecular dynamics on transputer arrays 1. Algorithm design, programming issues timing experiments and scaling projections. *Mol. Phys.* **66**, 637 (1989).
[32] M.R.S. Pinches, D.J. Tildesley and W. Smith. Large scale molecular dynamics on parallel computers using the linked-cell algorithm. *Mol. Simulations* **6**, 51–87 (1991).
[33] K. Esselink and P.A.J. Hilbers. Efficient parallel implementation of molecular dynamics on a toroidal network: Part II multi-particle potentials. *J. Comp. Phys.* **106**, 108–114 (1993).
[34] B. Smit, P.A.J. Hilbers, K. Esselink, L.A.M. Rupert, N.M. van Os and A.G. Schlijper. Structure of a water/oil interface in the presence of micelles: a computer simulation study. *J. Phys. Chem.* **95**, 6361–6368 (1991).
[35] B. Smit, P.A.J. Hilbers and K. Esselink. Computer simulations of simple oil/water/surfactant systems. *Tenside Surf. Det.* **30**, 287–293 (1993).
[36] A.C. Balazs, Z. Zhoe and C. Yeung. Behaviour of amphiphilic comb copolymers in oil/water mixtures: a molecular dynamics study. *Langmuir* **8**, 2295–2300 (1992).
[37] A.Z. Panagiotopoulos. Direct determination of phase coexistence properties of fluids by Monte Carlo simulation in a new ensemble. *Mol. Phys.* **61**, 813–826 (1987).
[38] B. Smit. "Computer simulations in the gibbs ensemble." In *Computer simulation in Chemical Physics*, M.P. Allen and D.J. Tildesley, editors, 173–209, Dordrecht, 1993. NATO ASI, Kluwer.
[39] J.I. Siepmann and I.R. McDonald. Monte Carlo simulation of the mechanical relaxation of a self-assembled monolayer. *Phys. Rev. Lett.* **70**, 453–456 (1993).
[40] J.I. Siepmann and I.R. McDonald. Monte Carlo study of the properties of self-assembled monolayers formed by the adsorption of $CH_3(CH_3)_{15}SH$ on the (111) surface of gold. *Mol. Phys.* **79**, 457–473 (1993).
[41] G.C.A.M. Mooij, D. Frenkel, and B. Smit. Direct simulation of phase equilibria of chain molecules *J. Phys.: Condens. Matter* **4**, L255–L259 (1992).
[42] M. Laso, J.J. de Pablo and U.W. Suter. Simulation of phase equilibra for chain molecules. *J. Chem. Phys.* **97**, 2817–2819 (1992).
[43] J.I. Siepmann, S. Karaborni and B. Smit. Simulating the critical properties of complex fluids. *Nature* **365**, 330–332 (1993).
[44] J.I. Siepmann, S. Karaborni and B. Smit. Vapor–liquid equilibria of model alkanes. *J. Am. Chem. Soc.* **115**, 6454–6455 (1993).
[45] W.L. Jorgensen, J.D. Madura and C.J. Swenson. Optimized intermolecular potential function for liquid hydrocarbons. *J. Am. Chem. Soc.* **106**, 6638–6646 (1984).
[46] C. Tsonopoulos. Critical constant of normal alkanes from methane to polyethylene. *AIChE Journal* **33**, 2080–2083 (1981).
[47] B.D. Smith and R. Srivastava. *Thermodynamics data for pure compounds: Part A hydrocarbons and ketones.* Elsevier, Amsterdam, 1986.